



The Egyptian International Journal of Engineering Sciences and Technology

Vol. 27 (2019) 30–42

<http://www.eijest.zu.edu.eg>



Vibration Signature of Misaligned Rotors of Centrifugal Pump

Ahmed H. Osmana*, Ahmed Abd Elbar Salman, Khaled M. Fawzy

Zagazig university, Zagazig, 44519, Egypt

ARTICLE INFO

Article history:

Received 11 July 2018
Received in revised form
21 Feb. 2019
Accepted 08 March 2019
Available online 10 March
2019

Keywords:

Centrifugal Pump
Misalignment
FFT
Vibration Signature
Vibration Analysis

ABSTRACT

The cost of breakdown of rotating machines such as centrifugal pumps encouraged the industrial sector to develop technics for early fault detection. Vibration analysis is a powerful tool to diagnose the problem. It's used for fault diagnosis and distinguishing the fault types at an early stage, where each faulty element has its exciting frequencies. This paper focus on the shafts' misalignment. This fault is one of the most common problems that can be found in pumping stations. Misalignment is the condition where the two shafts of the drive and driven machine are not on the same centerline. More vibration and excessive forces in the bearing area are generated due to the misaligned rotors. Two cases were measured on a centrifugal pump to predict the vibration signature due to shaft's misalignment. The studied system consists of one stage centrifugal pump driven by a motor with rated power 55 kW @ 2980 rpm and flexible type coupling. FFT analyzer is used to analyze the frequency spectrum of the vibration. Vibration data of the inspected pump is collected in the normal and abnormal conditions. The vibration signature of both cases is compared with ISO10816. It has been found that the shaft misalignment causes high peaks at 1X, 2X, and 3X. The amplitude of the 2X vibration is higher than that of the 1X, when misalignment is parallel and lower than 1X, when misalignment is angular. The experimental results obtained from this study gave more understanding on the effective role of vibration analysis in predicting and diagnosing machine faults.

1. Abbreviations

A	Axial	MNDE	Motor Non Drive End
DE	Drive End	NDE	Non Drive End
DSS	Deflected Shaped Shaft	PDE	Pump Drive End
FFT	Fast Fourier Transformation	PNDE	Pump Non Drive End
H	Horizontal	RMS	Root Mean Square
		1X	1 st order of the frequency
HP	High Pressure	Rpm	Revolution Per Minute
MDE	Motor Drive End	V	Vertical

* Corresponding author. Tel.: +201027637525
Email address: ahamdy@hotmail.com

2. Misalignment

Shaft misalignment is incorrect alignment, occurs when the centerlines of the motor and the driven equipment shafts are not in line with each other. Shaft misalignment has major implications for rotating equipment reliability. Although on the wide range a lot of effective alignment techniques are successfully applied to equipment, sometime deterioration of the alignment occurs due to, changing equipment operating conditions, settlement of foundation or piping strain. Which results excessive forces on the rotating equipment. This lead to coupling or bearing failure.

There are basically three types of misalignment:

- Angular misalignment
- Parallel misalignment
- General misalignment (combination of parallel and angular).

2.1 Angular misalignment

The angular misalignment occurs when the centerline of the two shafts meets each other at a certain angle, shown in Fig1. When a bending moment on each shaft occurs, a strong vibration at 1X and some vibration at 2X in the axial direction at both bearings will be generated. Also there will be fairly strong radial and/ or transverse 1X and 2X levels in the opposite phase [7]. In this case, the vibration on both bearings will be in phase. Usually, misaligned coupling produces at the bearings on the other ends of the shafts fairly high axial 1X levels, as shown Fig 2.

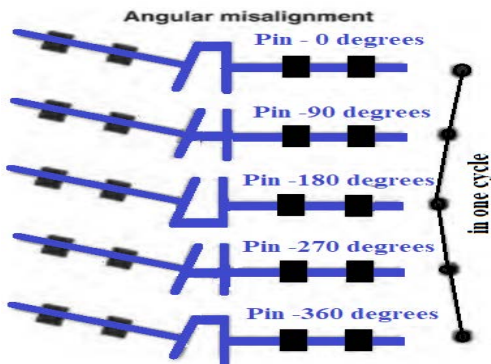


Fig. 1: Angular misalignment [7]

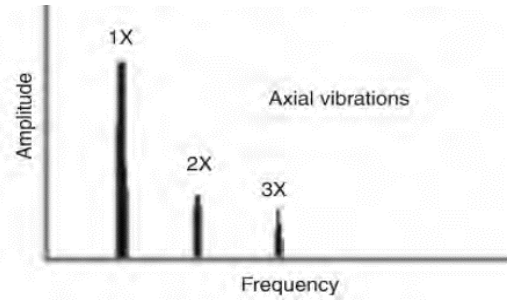


Fig. 2: FFT of angular misalignment [7]

Often, dominant angular misalignment and a bent shaft give similar FFT vibration signatures. In both the radial and axial direction [7]. The bent shaft case are noticed on the two bearings of the same shaft of the machine this indicate, that there is a phase difference. On the other hand, the phase difference appears on the bearing across the coupling when measuring the axial phase on the bearings of the two machines across the coupling a 180° phase difference, as shown in Fig 3.

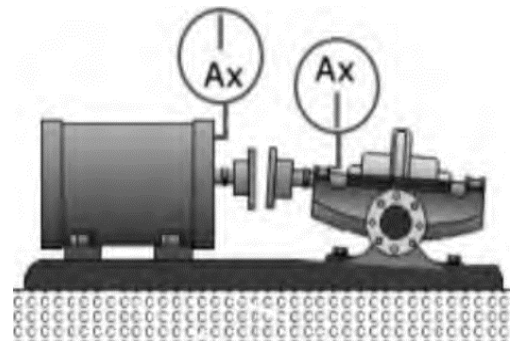


Fig. 3: Angular misalignment confirmed by phase analysis

2.2 Parallel misalignment

Parallel misalignment occurs when the centerlines of both shafts of the two machines are parallel to each other and there is an offset between them. Parallel misalignment is shown in Fig 4.

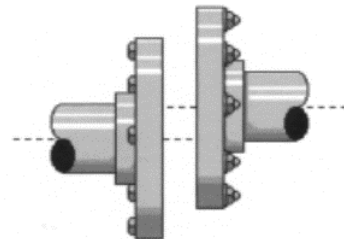


Fig. 4: Parallel misalignment

Parallel misalignment and angular misalignment have similar vibration symptoms but the parallel misalignment shows higher vibration in the radial direction and there will be a 180° phase difference across the coupling [7]. It's rare to find pure parallel misalignment but it is commonly observed to be conjunction with angular misalignment. Thus, the 1X and 2X peaks will be clearly identified. When the parallel misalignment is predominant, 2X is often larger than 1X [7]. The peaks with high amplitudes @ harmonics [3X to 8X] are shown in Fig 5 even a whole series of high-frequency harmonics are generated when a severe either parallel and angular misalignment occurring. Coupling construction will often significantly influence the shape of the vibration signature if the misalignment is severe, as shown in Fig 6.

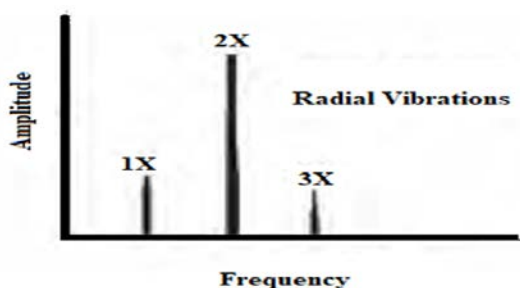


Fig. 5: FFT of parallel misalignment [7]

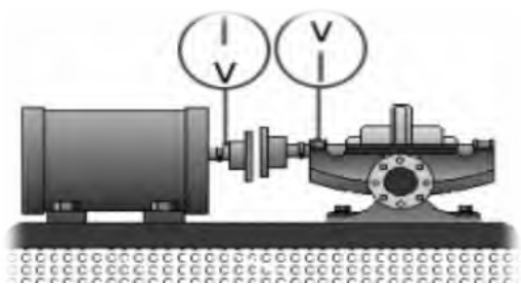


Fig. 6: Radial phase shift of 180° is observed across the coupling

2.3 General Misalignment

In most cases of misalignment there are combination of the two above described types, as shown in Fig 7. The diagnosis is based on the existence of 1X and 2X axial peaks and on stronger 2X peaks than 1X peaks. The high axial 1X levels are not caused by an imbalance in overhung rotors [7].

Accordingly misalignment produces variety of symptoms on different types of machines, and the average vibration signatures for healthy machines should be consulted to determine allowable 1X and 2X levels.

3. Introduction

Irvin Redmond [1] showed that both the static and dynamic multi-harmonic system response can be produced due to misalignment. Also the torsional response that mainly occurred at the fundamental and second harmonic frequencies can introduce at the parallel offset. Axial thrust force, which dominated by 1X (running speed) and 2X (two time running speed) response is induces from parallel misalignment. Support anisotropy plays a major role in determining system dynamic response. The dynamic response increases with greater divergence of support orthogonal stiffness value. larger parallel offset leads to an increase in system dynamic at 1X (running speed) and 2X (two time running speed).

Mohsen Nakhaeinejad and et al. [2] showed that vibrations and forces of a machine with rigid coupling are more sensitive to the parallel misalignments than angular misalignments. Regarding the axial forces, higher forces with more variations can be generated in a misaligned rotor coupled with a helical beam coupling than rigid coupling. Investigating the axial forces in frequency-domain reveals significant 3X (three time running speed) and 5X (five time running speed) harmonics for angular and 3X (three time running speed) and 6X (six time running speed) harmonics for parallel misalignments.

Vaggeeram Hariharan and et al. [3], carried out simulation and experimental studies for the rigid and pin type flexible coupling with parallel misalignment shaft. They found that the obtained frequency spectra are similar and the results prove that misalignment can be characterized primarily by second harmonics 2X of the shaft running speed.

Seema Nagrani, S. S. Pathan, and et al. [4], carried out test on a reactor system, which runs on an induction motor. They found that the misalignment fault occurs at the running frequency and its harmonics. The maximum peak occurs at the 1X frequency. They concluded that analysis of vertical and axial directions are important for the angular misalignment.

K. Venkata Sivarao, et al. [5] used the motor

current signature analysis to determine the misalignment. The measurements that detect the misalignment of the motor and the machine shafts had been taken at full load and no load conditions. The experimental study demonstrates that misalignment represents type of load on motor, where the current (in Amperes) increases with the increase of the load. Peak amplitudes are observed at 1X (running speed) in the axial direction. Guang Meng and et al. [6] investigated theoretically and experimentally the dynamic response of a multi-disk rotor system with coupling misalignment. They found that the experimental and theoretical studies are matching together. This study shows that misalignment can cause multiple frequency vibrations including 2X (two time running speed), 3X (three time running speed), 4X (four time running speed) and 5X (five time running speed). The other multiple frequency components of vibration, among which the 2X (two time running speed) vibration is dominant and misalignment does not change the first critical speed of the rotor system. Verma and et al, [8], inspected the different types of misalignments by using diagnostic medium such as stator current signature as well as rotor vibration signal. It has been found that current signature alone can predict the misalignment effect without use of vibration signal. Orbit plots are effectively used to explain the unique nature of misalignment fault. Shaft displacement and stator current samples during machine run up under aligned and misaligned conditions are measured and analysed. Result shows that misalignment is the parameter that is more responsible for the cause of instability. Changrui Bai et al, [9] present the results of vibration data analysis and outline an approach for vibration analysis of the shaft/coupling misalignment of rotating machines. This includes uses of rotor frequency response function and physics based predictive model.

Nader Sawalhi and et al, [10] presents a detailed finite element and dynamic simulation model of a vibration test rig. Both simulated and experimental results exhibited similar behaviour. An increase of lower and higher harmonics of the shaft speed of the acceleration vibration signal was observed with smearing noticed at higher orders. A low-frequency modulation was reported in the measured signal with similar behaviour captured in the simulated signal. Further investigation still needs to be carried out to provide a solid understanding of this interaction.

4. Misalignment Problem of a Pumping System

Figure 8 shows the feed pump which used in this study. Fig. 8b shows Schematic drawing of the pumping system. In this case, the measurements are carried out at the normal and faulty conditions. The pump consists of three stages and is driven using an electric motor. The motor speed is 2980 rpm and its rated power is 200 kW. This pumping system is used to pumping crude oil. Vibration readings for both the detected and normal case are taken on the bearings. The defects are identified through vibration analysis by finding the difference in amplitudes. Overall vibration levels are measured and analyzed at both, the normal and faulty conditions during different periods. The measurements are compared with ISO 10816.

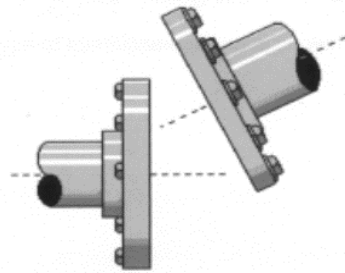


Fig. 7: Coupling with most common form of misalignment



Fig. 8a: Feed pump

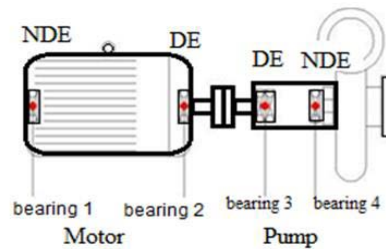


Fig. 8b: Schematic drawing for Figure 8a

4.1 Measurements at normal condition

The vibration signature of the healthy pump is recorded. This signature is used as a baseline data for future analysis. This vibration signature is shown in the Fig 9, 10, 11 and 12. The signal is measured at three directions (axial, vertical and horizontal) for the pump and motor’s bearings at both the drive end "DE" and non-drive end "NDE". The graphs show normal overall readings for all bearings.

Table 1 shows the measured amplitude readings of the normal and faulty operations at the four positions of the pump system (Motor NDE, Motor DE, Pump DE and Pump NDE) at the three axes (vertical, horizontal and axial). These readings are compared with both alarm and critical limits. It’s obviously that these readings are normal.

The results are presented in three axes (A, V and H). The horizontal axis of the figure represents the order

Table 1 the normal and faulty overall reading

Normal	Motor NDE			Motor DE			Pump DE			Pump NDE		
	V	H	A	V	H	A	V	H	A	V	H	A
Unit	mm/s RMS	mm/s RMS	mm/s RMS	mm/s RMS	mm/s RMS	mm/s RMS	mm/s RMS	mm/s RMS	mm/s RMS	mm/s RMS	mm/s RMS	mm/s RMS
Alarm	4.5	4.5	4.5	4.5	4.5	4.5	4.5	4.5	4.5	4.5	4.5	4.5
Critical	7	7	7	7	7	7	7	7	7	7	7	7
Normal	1.57	0.877	0.997	1.31	0.999	0.876	0.979	0.83	1.32	0.896	0.82	0.899
Faulty	7.9	23.21	13.1	19.04	17.53	22.88	21.58	14.14	18.41	14.62	28.59	10.59

of frequencies and the vertical axis represents the amplitude in mm/s.

The vertical scale is changed according to the maximum value to clearly see its magnitude. Figure 9 shows the spectrum of the motor at the DE. It’s obviously that the amplitude (0.67 mm/s) in the vertical direction at (1X) is the highest amplitude. This represents a normal case.

Fig 10 shows the spectrum of the motor at the NDE. The amplitude (1.35mm/s) in the vertical direction at (2X) is the highest amplitude. This case represents a normal case.

Fig 11 shows the spectrum of the pump at the DE. The amplitude (0.83 mm/s) in the axial direction at (2X) is the highest amplitude. This case represents a normal case.

Fig 12 shows the spectrum of the pump at the NDE. The amplitude (0.67 mm/s) in vertical Direction is the maximum amplitude at (2X)

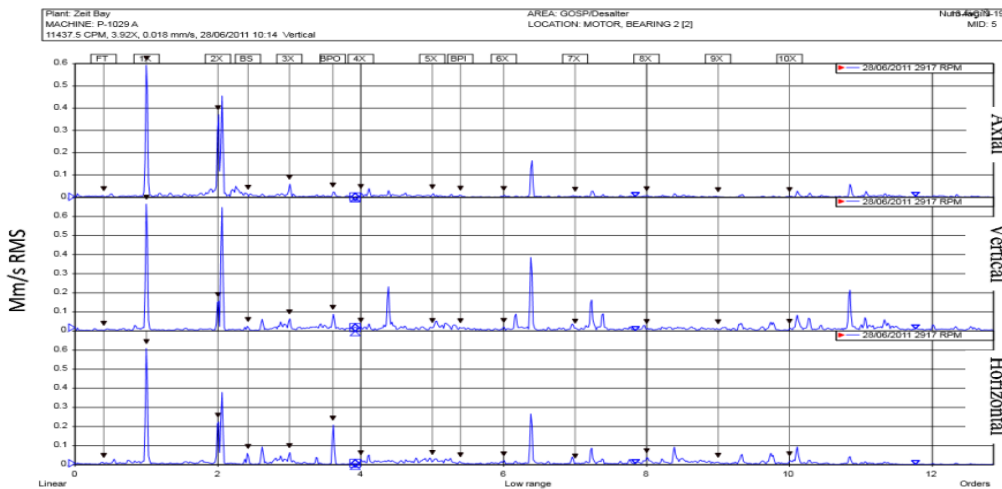


Fig. 9: Normal vibration signature of motor DE

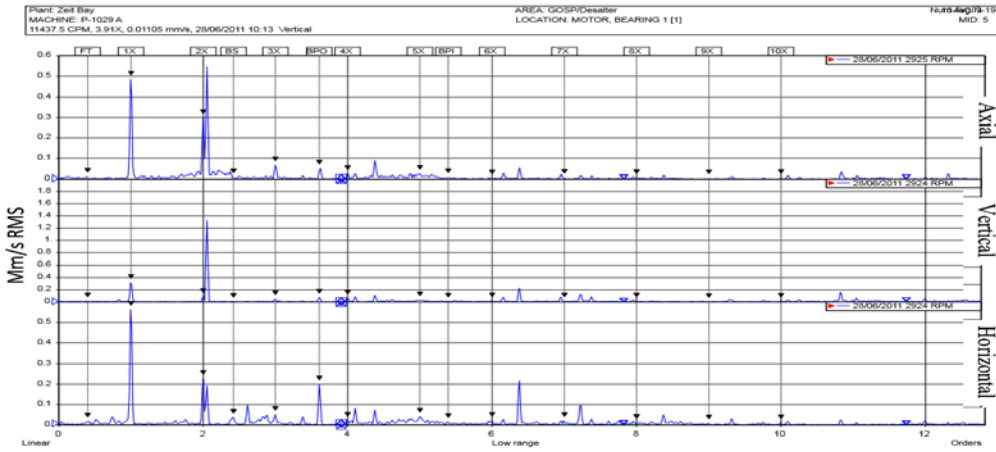


Fig. 10: Normal vibration signature of motor NDE

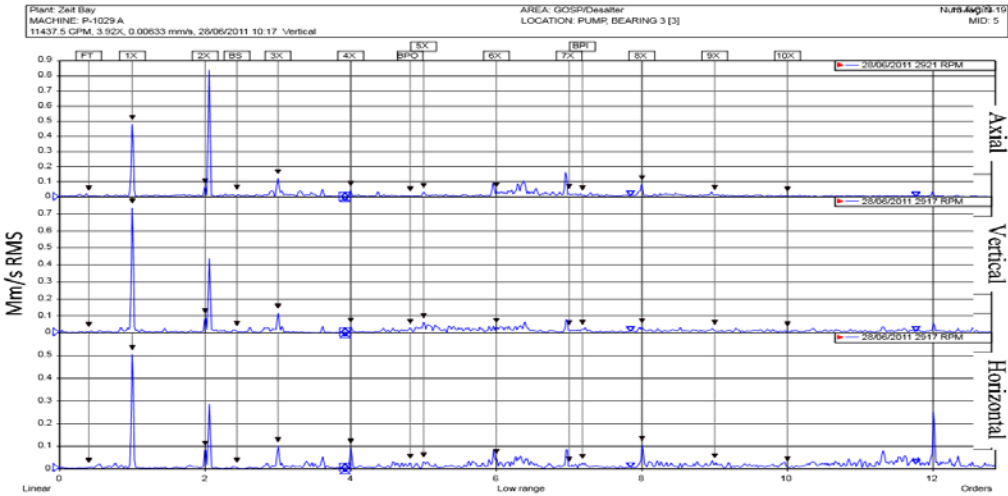


Fig. 11: Normal vibration signature of pump DE

4.2 Measurements at abnormal condition

Fig 13 shows the spectrum of the motor at the DE. There is a noticeable increase in the amplitude at 1X which equals (17.2 mm/s at the axial, 6.1 mm/s at the vertical and 8.9 mm/s at the horizontal direction) and 2X equals (11.1 mm/s at the axial, 15.2 mm/s at the vertical and 9.8 mm/s at the horizontal).

Fig 14 shows the spectrum of the motor at the NDE. There is a noticeable increase in the amplitude of 1X equals (10.1 mm/s at the axial, 1.1 mm/s at the vertical and 7.8 mm/s at the horizontal direction) and 2X equals (4.1 mm/s at the axial, 4.2 mm/s at the vertical and 16.1 mm/s at the horizontal direction).

Fig 15 shows the spectrum of the pump at the DE. It can be noticed that, there are extremely rising in the amplitude of 1X equals (3.9 mm/s at the axial, 9.9 mm/s at the vertical and 3.2 mm/s at the horizontal direction) and 2X equals (15.1 mm/s at the axial, 15.1 mm/s at the vertical and 9.8 mm/s at the horizontal directions).

Fig 16 shows the spectrum of the motor at the DE. It's can be seen that there is an increase in the amplitude at 1X equals (2.1 mm/s at the axial, 5.6 mm/s at the vertical and 2.1 mm/s at the horizontal directions) and 2X equals (8.1 mm/s at the axial, 6.8 mm/s at the vertical and 11.1 mm/s at the horizontal directions).

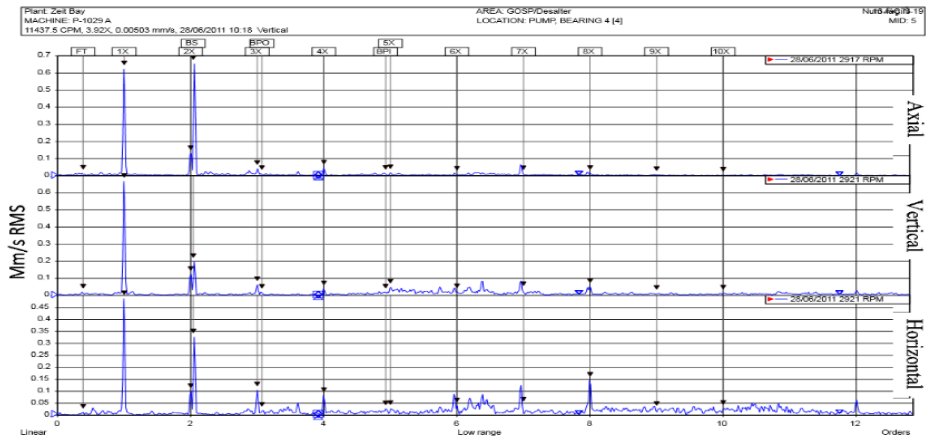


Fig. 12: Normal vibration signature of pump NDE

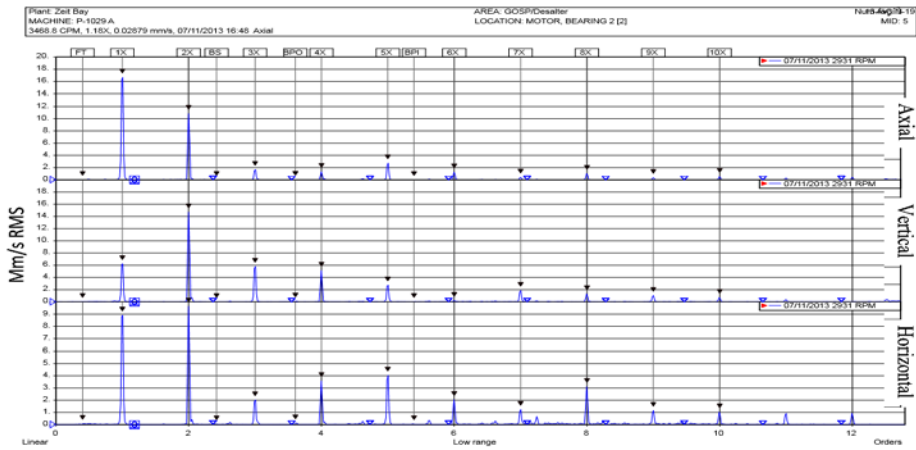


Fig. 13: Abnormal vibration signature of motor DE

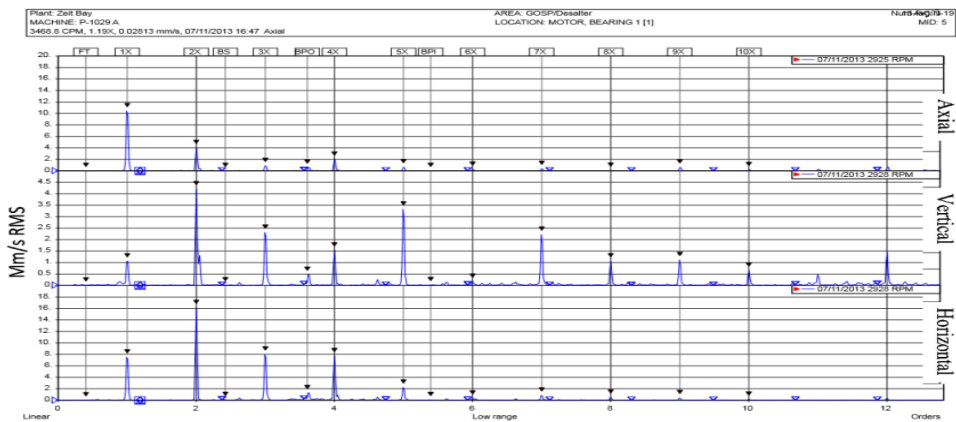


Fig. 14: Abnormal vibration signature of motor NDE

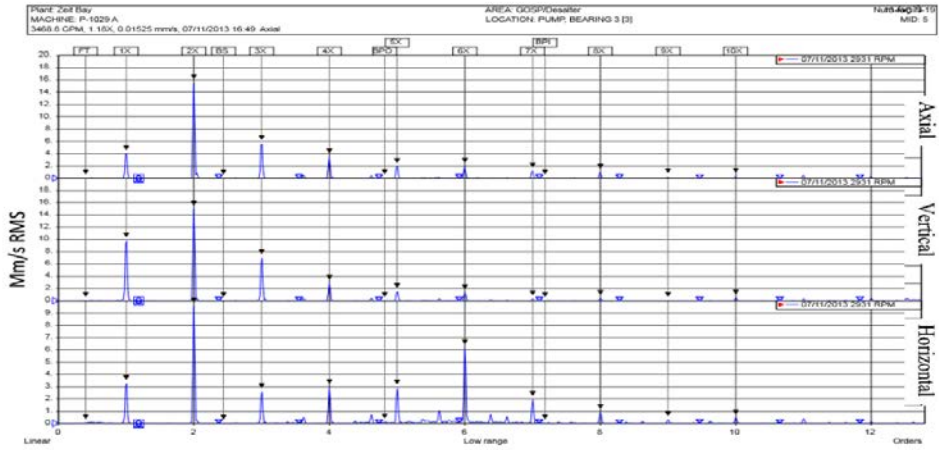


Fig. 15: Abnormal vibration signature pump DE

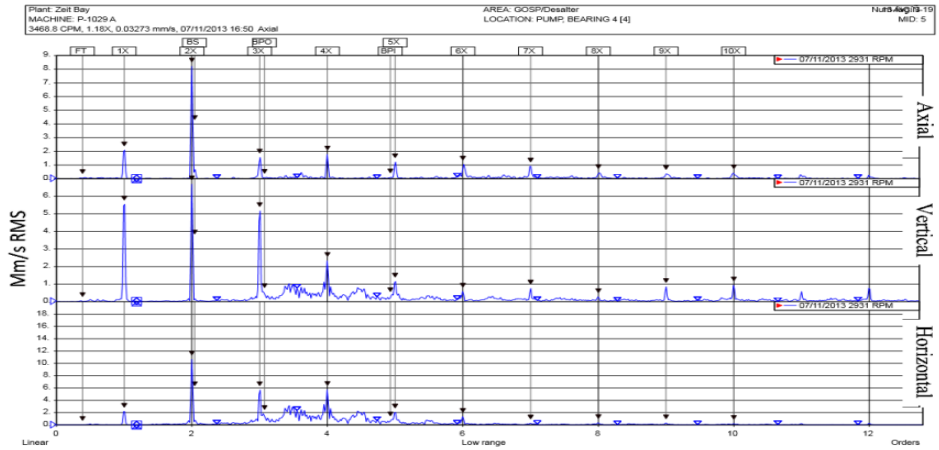


Fig. 16: Abnormal vibration signature of pump NDE

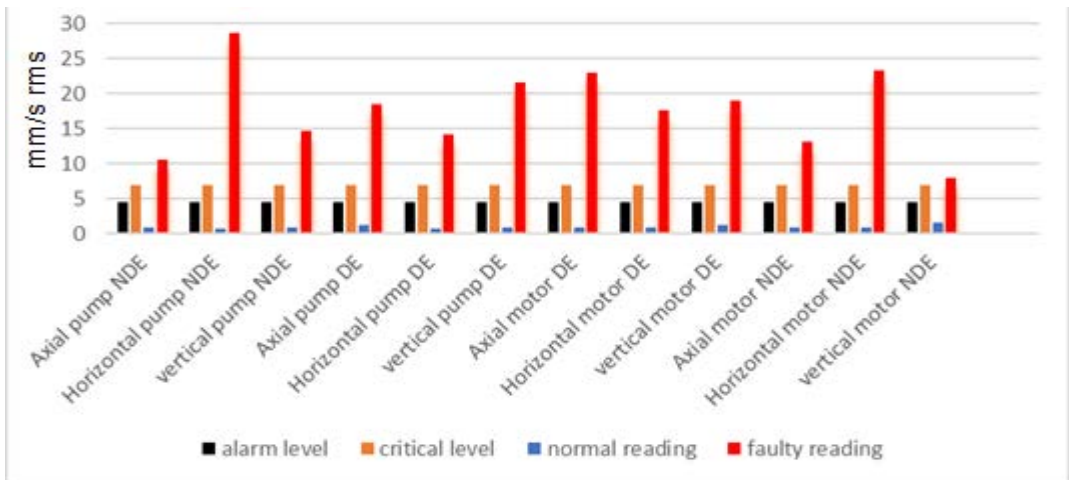


Fig. 17: Comparison between alert level, critical level, normal and abnormal overall reading

4.3 Comparison between normal and abnormal conditions

Refereeing to Table 1 to see the comparison between alert levels, critical levels, normal and abnormal overall readings. The data are compared at the four positions of the pumping system (Motor NDE, Motor DE, Pump DE and Pump NDE) at the three axes (V, H and A). The data in this table is plotted on Fig 17. The comparison between normal and abnormal cases are shown in Figs 18, 19, 20, and 21, where the red color represents the faulty case and the blue color represents the normal case. As it can be shown that a large difference between the normal

readings and faulty readings.

Figure 17 shows the comparison between the alarm levels (black color), the critical levels (orange color), overall readings (blue color) and the abnormal reading (red color). The figure shows that the height of the faulty readings compared with the normal readings together with the alarm and critical limits.

Figs 18, 19, 20, and 21 show a comparison between the normal spectra (blue color) and abnormal spectra (red color) at the four positions (Motor NDE, Motor DE, Pump DE and Pump NDE). There are extremely rising in the abnormal case in (1X) and (2X) than the normal case in the three directions.

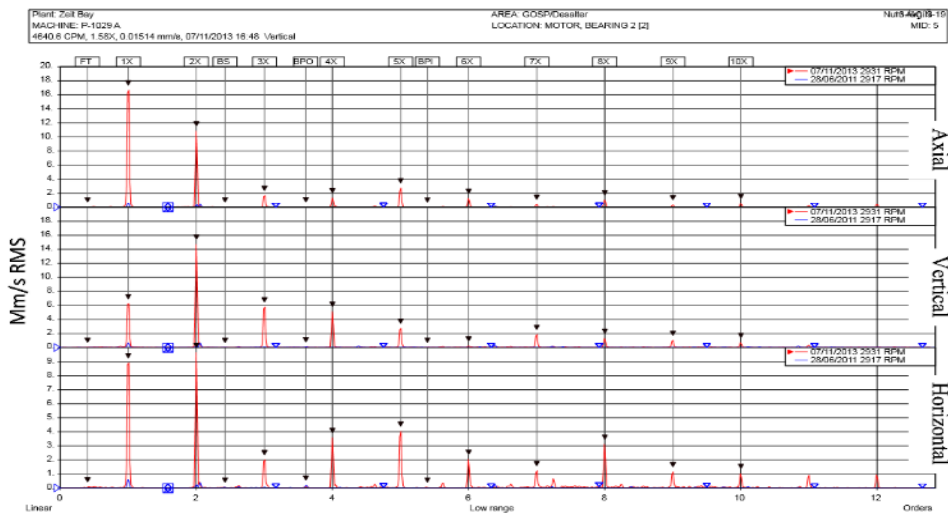


Fig. 18: Comparison between faulty & normal vibration signature of motor DE

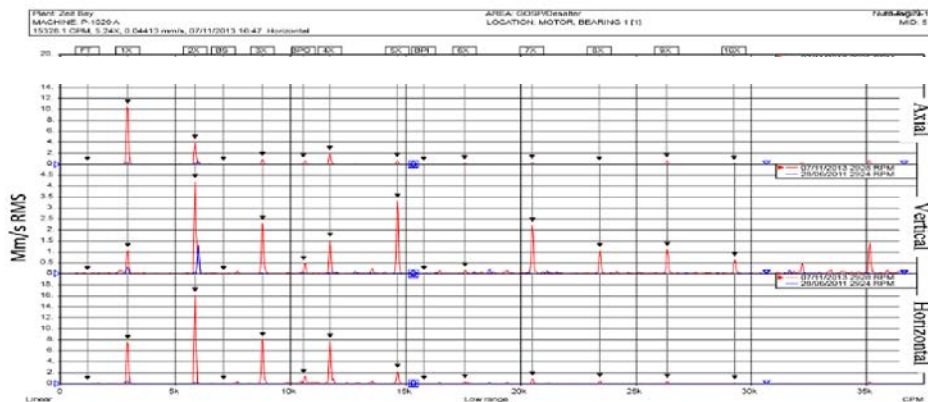


Fig. 19: Comparison between faulty & normal vibration signature of motor NDE

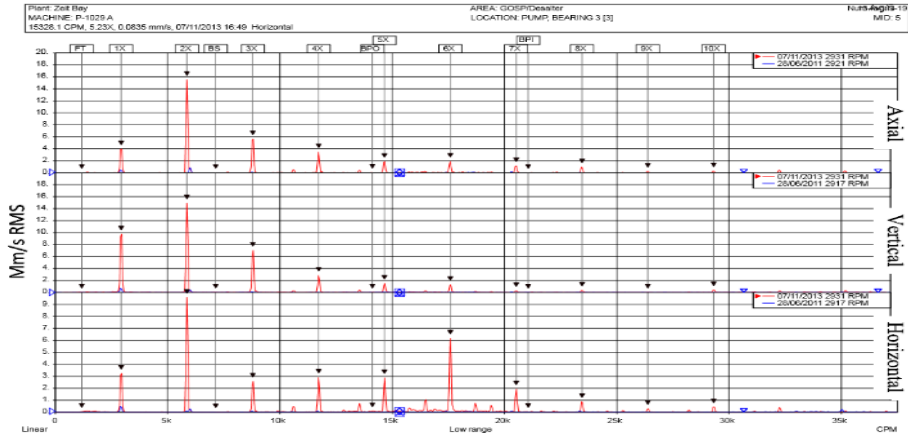


Fig. 20: Comparison between faulty & normal vibration signature of pump DE

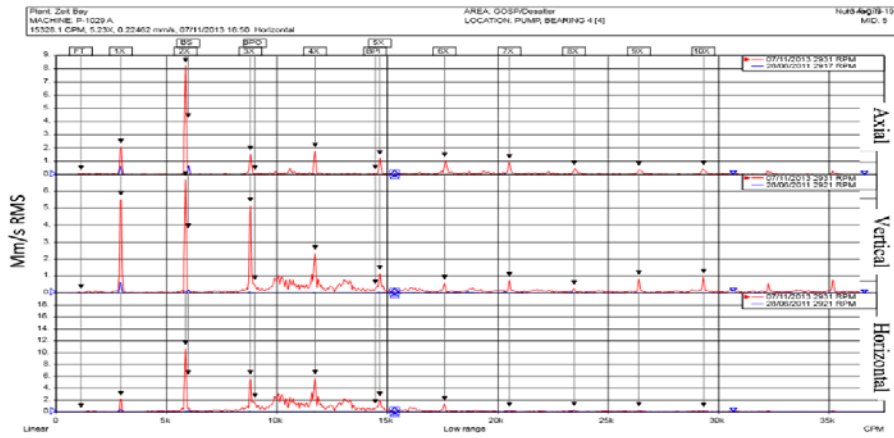


Fig. 21: Comparison between faulty & normal vibration signature of pump NDE

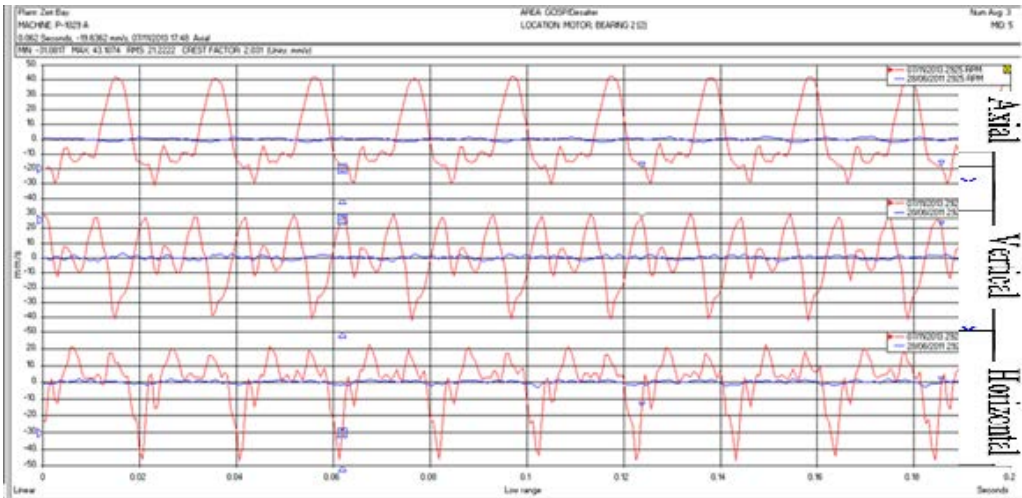


Fig. 22: Normal (blue) and abnormal (red) time waveform of motor DE

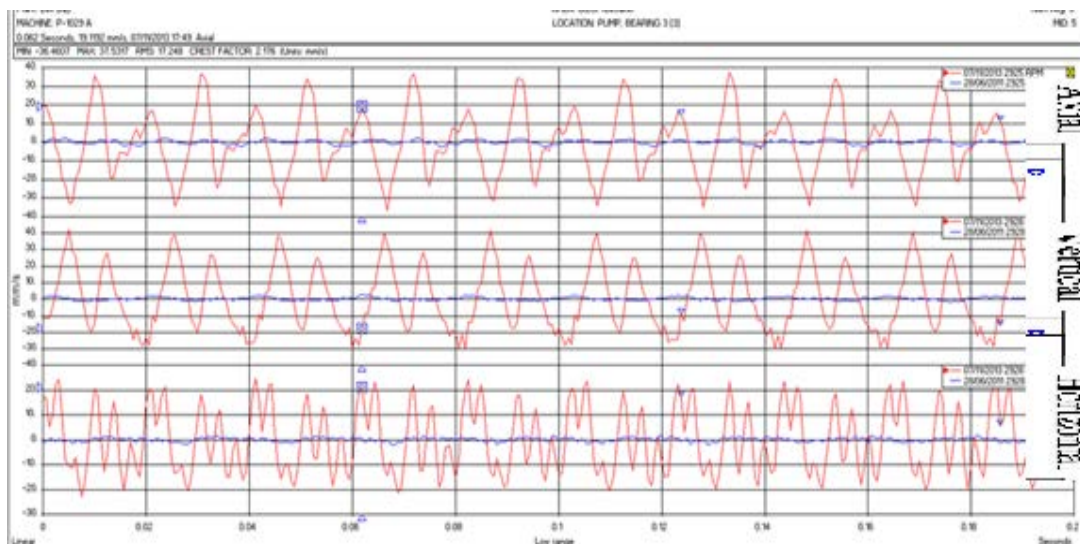


Fig. 23: Normal (blue) and abnormal (red) time waveform comparison of pump DE

Figure 22 shows a comparison between the normal time waveform (blue color) and abnormal time waveform (red color) for the Motor at the DE.

Figures 23 shows a comparison between the normal time waveform (blue color) and abnormal time waveform (red color) for the pump at the DE.

In both Figs 22 and 23, there is a noticeable difference between the normal and abnormal cases.

5. Finding and discussion

Vibration signatures, as shown in Fig. 18, 19, 20 and 21 show the maximum average amplitudes for all positions (Motor DE, Motor NDE, Pump DE and Pump NDE) in three directions (Axial, Vertical and Horizontal at 1X rpm (50 Hz).

The vibration signals are measured for both cases (normal and faulty) for all positions and it's found that: Reading the Motor bearing at the DE, the vibration signature demonstrates high peaks in the axial direction at 1X and 2XAs shown in Fig 18. The amplitude at 2X is lower than the 1X peak. As misalignment produces bending moment in each shaft, strong vibration is generated at 1X in the axial direction accordingly, angular misalignment is suspected. The vibration signature demonstrates high peaks at 1X, 2X, 3X, 5X in both horizontal and, vertical directions. It's clear that 2X vibration is higher than 1X. 1X and 2X are higher in vertical direction than 1X and 2X in horizontal direction

respectively at motor drive end. Also 1X and 2X are higher in horizontal direction than 1X and 2X in vertical direction respectively at motor non drive end. (This may happen along the same component (motor) at misalignment condition. The bending moment of each shaft of the coupled ends and shear force is produced from Parallel misalignment so parallel misalignment is suspected.

Regarding the Motor bearing at the NDE. The vibration signature at Fig19 demonstrates that strong 1X in horizontal direction. Also, 1X in vertical direction is higher in comparison with the normal reading. The amplitude of 1X in horizontal direction is fourth time the amplitude of the 1X in vertical direction. As the horizontal is the direction of greatest weakness, looseness is suspected at motor non drive end

The vibration signature demonstrates that ball pass frequency outer race increased in amplitude value than the normal reading and also high amplitudes at 1X and multiples 2X,3X,4X ...

Regarding the pump bearing at the DE, the vibration signature demonstrates high peaks at 1X, 2X, 3X, 5X in both horizontal and vertical direction, as shown in Fig 20. Also 2X vibration is higher than 1X. 1X and 2X are higher in the vertical direction than 1X and 2X in the horizontal direction respectively at motor drive end. Furthermore, 2X is higher in horizontal direction than 1X and 2X in vertical direction at motor non drive end. This may happen along the

same component (motor) at misalignment condition. Parallel misalignment produces both shear force and bending moment of each shaft of the coupled ends so parallel misalignment is suspected. All this are produced combined parallel and angular misalignment.

Regarding the pump bearing at the NDE, the vibration signature demonstrates high peaks at 1X, 2X, 3X in the horizontal direction. The peak at 2X is higher than the peak at 1X for the axial and vertical directions, as shown in Fig 21.

6.5 Time wave

The time waveform in Figs 22 and 23 show a classic symptoms of misalignment with “M” and “W” shapes. The comparison shows the difference between normal and faulty condition for the motor and pump.

6. Conclusions

Misalignment is common due to fault of alignment practices because of thermal growth, shifting foundation, pipe strain etc... The vibration doesn't always change in predictable ways when the shaft is misaligned. It is found from the case study that the shaft misalignment produces a high peak at 1X, 2X, 3X, 4X and 5X. The presence of 3X, 4X and 5X depends on the coupling type and degree of misalignment. In the parallel misalignment, 2X can be quite high compared to 1X vibration. The angular misalignment generates a bending moment on each shaft. This load is transferred to the bearings and consequently generates a strong vibration at 1X and vibration at the 2X in the axial direction. Misalignment may generate a shear force and bending moment on the coupled end of each shaft which may lead to failure

References

- [1] Irvin Redmond, "Shaft misalignment and vibration - A Model", Proceedings of the Society for Experimental Mechanics Conference, Saudi Aramco, PP. 118–124, 2007.
- [2] Mohsen Nakhaeinejad and SuriGaneriwala, "Observations on dynamic responses of misalignments", Spectra Quest Inc., 8201

Hermitage Rd, Richmond, VA 23228. 2009.

- [3] VaggeeramHariharan and PSS.Srinivasan, "Vibration analysis of parallel misaligned shaft with ball bearing system", Songklanakarini Journal Science and Technology, Vol. 33(1), PP. 61-68, 2011.
- [4] Seem Nagrani, S. S. Pathan, and I H Bhoraniya, "Misalignment fault diagnosis in rotating machinery through the signal processing technique – signature analysis", International Journal of Advanced Engineering Research and Studies, Vol.1(II), PP. 1-4,2012.
- [5] K. Venkata Sivarao, G. Diwakar and M. R. S. Satynarayana, "Determination of misalignment using motor current signature analysis in rotating machine ", (IJERT International Journal of Engineering Research & Technology, Vol. 1(8), PP. 1-12, 2012.
- [6] GuangMeng and Yang Yang, "Theoretical and experimental study on the dynamic response of multi-disk rotor system with flexible coupling misalignment", Journal of Mechanical Engineering, Vol. 266(12), PP. 2874-2886, 2012.
- [7] PareshGirdha, Cornelius Scheffer, "Practical Machinery vibration analysis and predictive maintenance", IDC Technologies, 2004.
- [8] Verma, Alok Kumar, Somnath Sarangi, and M. H. Kolekar. "Experimental investigation of misalignment effects on rotor shaft vibration and on stator current signature." Journal of Failure Analysis and Prevention 14.2 (2014): 125-138.
- [9] Bai, Changrui, SurendraSuriGaneriwala, and Nader Sawalhi. "A Rational Basis for Determining Vibration Signature of Shaft/Coupling Misalignment in Rotating Machinery." Rotating Machinery, Vibro-Acoustics & Laser Vibrometry, Volume 7. Springer, Cham, 2019. 207-217.
- [10] Sawalhi, Nader, SuriGaneriwala, and MátéTóth. "Parallel misalignment modeling and coupling bending stiffness measurement of a rotor-bearing system." Applied Acoustics 144 (2019): 124-141.

[11] ISO 10816-7 "Mechanical vibration -- Evaluation of machine vibration by measurements on non-rotating parts -- Part 7: Rotor dynamic pumps for industrial applications, including measurements on rotating shafts" International Organization for Standardization, part 7, 2009.

Appendix

VIBRATION SEVERITY PER ISO 10816					
Machine		Class I small machines	Class II medium machines	Class III large rigid foundation	Class IV large soft foundation
in/s	mm/s				
Vibration Velocity Vrms	0.01	0.28			
	0.02	0.45			
	0.03	0.71		good	
	0.04	1.12			
	0.07	1.80			
	0.11	2.80		satisfactory	
	0.18	4.50			
	0.28	7.10		unsatisfactory	
	0.44	11.2			
	0.70	18.0			
	0.71	28.0		unacceptable	
	1.10	45.0			